Distribution Agreement

In presenting this thesis as a partial fulfillment of the requirements for a degree from Emory University, I hereby grant to Emory University and its agents the non-exclusive license to archive, make accessible, and display my thesis in whole or in part in all forms of media, now or hereafter now, including display on the World Wide Web. I understand that I may select some access restrictions as part of the online submission of this thesis. I retain all ownership rights to the copyright of the thesis. I also retain the right to use in future works (such as articles or books) all or part of this thesis.

Andrew Hoover April 14, 2020

Comparative Ultrastructural Localization of the Glutamate Delta-1 Receptor Immunoreactivity between the Mouse and Monkey Striatum

by

Andrew Hoover

Dr. Yoland Smith
Adviser

Neuroscience and Behavioral Biology

Dr. Yoland Smith

Adviser

Dr. Rosa Villalba

Committee Member

Dr. Gillian Hue

Committee Member

2020

Comparative Ultrastructural Localization of the Glutamate Delta-1 Receptor Immunoreactivity between the Mouse and Monkey Striatum

By

Andrew Hoover

Dr. Yoland Smith

Adviser

An abstract of
a thesis submitted to the Faculty of Emory College of Arts and Sciences
of Emory University in partial fulfillment
of the requirements of the degree of
Bachelor of Science with Honors

Neuroscience and Behavioral Biology

2020

Abstract

Comparative Ultrastructural Localization of the Glutamate Delta-1 Receptor Immunoreactivity between the Mouse and Monkey Striatum
By Andrew Hoover

Prior research has demonstrated the importance of Glutamate Delta (GluD) receptors, a ionotropic glutamate receptor family that does not express typical ligand-gated fast-current flow, in the development, maintenance and plasticity of synaptic microcircuits in the cerebellar cortex. Although GluD2 is the main GluD receptor subtype expressed in the cerebellum, GluD1 is widely distributed in the mammalian brain, particularly in forebrain regions including the striatum. Recent findings from our laboratories have shown that the knockout of GluD1 expression in striatal neurons elicits cognitive deficits and disrupts the anatomical and functional integrity of the thalamostriatal system in mice. To further interpret these observations and extend our understanding of GluD1 function to the human brain, a detailed understanding of the cellular, subcellular and subsynaptic localization of striatal GluD1in primates and rodents is needed.

At the light microscopic level, striatal GluD1 immunoreactivity displayed a patchy pattern of distribution that coincided with the striosome/matrix compartmentation, but in an opposite fashion between mice and monkeys. While GluD1 was more heavily expressed in the striosomes than the matrix in the monkey caudate nucleus, the opposite was found in the mouse dorsal striatum. At the electron microscopic level, GluD1 immunoreactivity was preferentially expressed in dendritic shafts (47.9 ± 1.2% of total labeled structures), followed by glia (37.7 ± 2.5%), and dendritic spines (14.3 ± 2.6%) in the matrix of the mouse striatum. This pattern was not statistically different from the distribution of labeling in both the striosome and matrix compartments of the monkey caudate nucleus, with the exception of a small amount of GluD1-poistive unmyelinated axons and axon terminals. Pre-embedding immunogold staining revealed perisynaptic GluD1 labeling at putative axo-dendritic and axo-spinous glutamatergic synapses, extrasynaptic GluD1 immunoreactivity and intracellular GluD1 labeling apposed to the external surface of mitochondria. These data provide a basic map needed to further elucidate the role of GluD1 at striatal glutamatergic synapses, but also suggest possible GluD1 functions at extrasynaptic neuronal, glial and mitochondrial sites.

Comparative Ultrastructural Localization of the Glutamate Delta-1 Receptor Immunoreactivity between the Mouse and Monkey Striatum

By

Andrew Hoover

Dr. Yoland Smith

Adviser

A thesis submitted to the Faculty of Emory College of Arts and Sciences
of Emory University in partial fulfillment
of the requirements of the degree of
Bachelor of Science with Honors

Neuroscience and Behavioral Biology

2020

Acknowledgements

I would like to give special thanks to Susan Jenkins and Jean-Francois Pare for excellent technical assistance and for training me on the many protocols it takes to successfully prepare tissue for microscopy. I would also like to thank all of my committee members for their time and expertise. This work was supported by the NIH grant R01MH116003 and the Yerkes Center NIH/ORIP base grant (P51-OD011132).

Table of Contents

Abstract:

Prior research has demonstrated the importance of Glutamate Delta (GluD) receptors, a ionotropic glutamate receptor family that does not express typical ligand-gated fast-current flow, in the development, maintenance and plasticity of synaptic microcircuits in the cerebellar cortex. Although GluD2 is the main GluD receptor subtype expressed in the cerebellum, GluD1 is widely distributed in the mammalian brain, particularly in forebrain regions including the striatum. Recent findings from our laboratories have shown that the knockout of GluD1 expression in striatal neurons elicits cognitive deficits and disrupts the anatomical and functional integrity of the thalamostriatal system in mice. To further interpret these observations and extend our understanding of GluD1 function to the human brain, a detailed understanding of the cellular, subcellular and subsynaptic localization of striatal GluD1in primates and rodents is needed.

At the light microscopic level, striatal GluD1 immunoreactivity displayed a patchy pattern of distribution that coincided with the striosome/matrix compartmentation, but in an opposite fashion between mice and monkeys. While GluD1 was more heavily expressed in the striosomes than the matrix in the monkey caudate nucleus, the opposite was found in the mouse dorsal striatum. At the electron microscopic level, GluD1 immunoreactivity was preferentially expressed in dendritic shafts (47.9 ± 1.2% of total labeled structures), followed by glia (37.7 ± 2.5%), and dendritic spines (14.3 ± 2.6%) in the matrix of the mouse striatum. This pattern was not statistically different from the distribution of labeling in both the striosome and matrix compartments of the monkey caudate nucleus, with the exception of a small amount of GluD1-poistive unmyelinated axons and axon terminals. Pre-embedding immunogold staining revealed perisynaptic GluD1 labeling at putative axo-dendritic and axo-spinous glutamatergic synapses, extrasynaptic GluD1 immunoreactivity and intracellular GluD1 labeling apposed to the external surface of

mitochondria. These data provide a basic map needed to further elucidate the role of GluD1 at striatal glutamatergic synapses, but also suggest possible GluD1 functions at extrasynaptic neuronal, glial and mitochondrial sites.

1. Introduction

It has been recently shown that the Glutamate Receptor Delta 1 (GRID1) promoter may possibly be a major contributor to disorders such as schizophrenia, bipolar behavior, or depression in rodent animal models (Treutlein et al. 2009; Benamer et al. 2018; Nakamoto et al. 2020). The association of GRID1 to these phenotypes is thought to be the result of the loss of its product – the delta 1 Glutamate receptor channel (GluD1). GluD1 is a ionotropic receptor channel that does not exhibit the typical fast ligand-gated ion flow (Kakegawa et al. 2007; Suryavanshi et al. 2016). It was originally discovered in the cerebellum alongside its relative GluD2, which has been well characterized in previous literature as being responsible for the development, maintenance and regeneration of parallel fiber synapses on Purkinje cells (Hirano. 2012; Ichikawa et al. 2016; Berridge et al. 2018; Pernice et al. 2019; Nakamoto et al. 2020). Given GluD2's role in the cerebellar cortex, it has been assumed that GluD1 may be necessary for the pruning and regulation of dendritic spines in other brain regions such as the hippocampus, the central nucleus of the amygdala or the striatum, which also exhibit high levels of the receptor (Suryavanshi et al. 2016). Recent data support this hypothesis, showing a higher density of dendritic spines on pyramidal neurons within the medial prefrontal cortex and CA1 region of the hippocampus in 30-day old GRID1 KO mice (Gupta et al. 2015). Glutamatergic delta receptors, like GluD1, exhibit their synaptic effects by collaborating with other presynaptic proteins to build a molecular bridge between terminal and postsynaptic element.

Cerebellin-1 (Cbln1) is a presynaptic glycoprotein first discovered in the cerebellum, where it consistently formed associations with GluD2 and worked in concert with GluD2 as a crucial synaptic organizer for Purkinje cells (Otsuka et al. 2016; Kusnoor et al. 2010) along with another presynaptic protein known as Neurexin (Nxn). Nxn is a presynaptic organizer protein that

binds to postsynaptic and intermediary elements (Uchigashima et al. 2019; Kakri et al. 2019). Together, GluD2, Nxn, and Cbln1 form a tripartite molecular complex that spans the synapse and forms a physical anchor for the pre and postsynaptic elements. This bridge helps new synapses form and maintains contact between the two elements (Uemura et al. 2010). There is evidence that Cbln1 and Nxn form similar synaptic bridges with GluD1 within the striatum (Yuzaki. 2018; Liu et al. 2020).

Our current understanding of GluD1 function in the CNS is limited by the lack of knowledge of its cellular and ultrastructural localization within the mammalian brain. In a recent study, Liu and colleagues (2020) demonstrated strong GluD1 expression within the mouse dorsal striatum and provided evidence for a GluD1-mediated regulation of the thalamostriatal projection from the parafascicular nucleus (Pf). They further showed that knockout of striatal GluD1 expression elicits cognitive deficits (Liu et al. 2020). To help address the underlying substrate of these promising findings, we undertook a detailed light and electron microscopic analysis of the cellular and sub-cellular localization of GluD1 in the mouse dorsal striatum. Furthermore, we compared the pattern of striatal GluD1 expression between mouse and monkey striatum to help extend our understanding of GluD1 structure/function to the human brain.

2. Materials and Methods

2.1 Animals

Five wild-type mice were provided by Dr. Shashank Dravid at the University of Creighton School of Medicine and three adult male rhesus macaque monkeys were taken from the Yerkes National Primate Research Center breeding colony (see details in Tables 1,2). All animals were anesthetized with an overdose of pentobarbital and perfused with a Ringer solution followed by a mixture of paraformaldehyde (4%) and glutaraldehyde (0.1%). After perfusion, the brains were taken out from the skull, cut in 10-15 mm thick blocks and post-fixed in 4% paraformaldehyde for 24 hours. The tissue blocks were then cut in 60 μm-thick coronal sections with a vibrating microtome. The housing, feeding, and experimental conditions used in these studies followed the guidelines for animal use and welfare set by the National Institutes of Health (National Research Council), and have been approved by Emory and Creighton University's Institutional Animal Care and Use Committees (IACUC).

2.2 Light Microscopy Immunocytochemistry

All commercially available primary antibodies used in this study have been well characterized and are listed in the Research Resources Identifiers (RRDIs) Portal (Table 3). The specificity of the GluD1 antibody has been further validated in our previous study by the lack of staining in the striatum of GluD1 KO mice (Liu et al. 2020) (see Table 3).

We first sought to examine GluD1 immunoreactivity at the LM level to determine if it followed any regional or compartmental pattern of distribution in the mouse and monkey striatum. Series of brain sections from the pre-commissural striatum of the mouse RM-119 and the monkey MR-272L were immunostained for GluD1. To determine if GluD1 immunoreactivity displayed

any relationships with the striosome/matrix striatal compartments, adjacent sections were labeled for either calbindin D28k (in monkey) or mu opioid receptors (in mice) to delineate the striatal compartments. The tissue was first placed in a sodium borohydride (1% PBS) solution for 20 minutes before being washed five times in phosphate buffered saline (PBS, 0.1 M, pH 7.4). Sections were then submerged in a pre-incubation solution for 60 minutes at room temperature (RT). The pre-incubation solution consisted of 1% normal animal serum (goat for GluD1/mu opioid receptor (MOR) and horse for calbindin), 1% Bovine Serum Albumin (BSA), PBS, and a 0.3% Triton-X-100 solution. After being submerged in pre-incubation, sections were incubated in the primary antibody solution of 1% normal animal serum, 1% BSA, primary antibody, and 0.3% Triton at room temperature (RT) for 24 hours. Following the primary antibody incubation, sections were washed in PBS and placed in a secondary antibody solution consisting of 1% normal animal serum, 1% BSA, secondary biotinylated antibody raised against the primary antibodies, and 0.3% Triton at RT for 90 minutes. Sections were washed again in PBS thoroughly before being placed in a Avidin-Biotinylated-Complex (ABC) solution for 90 minutes. The tissue was rinsed twice with PBS and once with tris(hydroxymethyl)aminomethane (TRIS, 0.05M, pH 7.6). GluD1 immunoreactivity was then revealed in a Diaminobenzidine (DAB, Sigma, St Louis, MO) solution made up of 48.5mL TRIS, 0.5mL imidazole (1.0M, Fisher Scientific, Norcross, GA), 0.025% DAB, and 1mL of hydrogen peroxide (0.3%). The DAB reaction occurred for 10 minutes before being stopped by several PBS washes. Sections were then mounted onto slides and cover slipped for later use.

2.3 Electron Microscopy Immunocytochemistry

Pre-embedding Immunoperoxidase

Brain sections from the pre-commissural striatum of 3 mice and 3 monkeys were processed for GluD1 localization at the electron microscopic level (see Tables 1,2). The tissue was first placed into a sodium borohydride (1% PBS) solution for 20 minutes and washed several times in PBS. Sections were then submerged in a cryoprotectant solution at RT for 20 minutes before being taken out and placed into a -80^{o}C freezer for another 20 minutes. Following this, sections were reintroduced to a 100% cryoprotectant solution for 10 minutes and then substituted with PBS in a stepwise manner by diluting cryoprotectant with PBS. Sections were immersed in a pre-incubation solution for 60 minutes at RT. From this point, our staining methods were the same as those above described for the LM immunocytochemistry, with the exception that Triton was omitted from all incubation solutions, and the primary incubation period lasted for 48 hours instead of 24 hours. Following the DAB reaction, sections were transferred from a PBS solution to a phosphate buffer solution (PB, 0.1M, pH 7.4) by stepwise substitution of PBS with PB. The tissue was then post-fixed in a 1% osmium tetroxide solution for 20 minutes. Following washes in PB, the samples were dehydrated in a step-wise manner in 50-100% alcohol solutions before being placed in a propylene oxide solution. Uranyl acetate (1%) was added to the 70% alcohol to increase contrast of tissue in the electron microscope. The dehydrated sections were then embedded in resin, mounted onto an oil-coated slide and cover-slipped before being baked at 60^{o}C for 48 hours. Blocks of striatal tissue were then taken out from the slide with a razor blade, cut using a Leica UCT Ultracut ultra-microtome and mounted onto single slot Pioloform-coated cupper grids.

Pre-embedding Immunogold

To help further assess the subcellular and subsynaptic localization of GluD1, tissue sections from RM-12, RM-74, RM-76 and MR-272L were processed for pre-embedding immunogold

staining. Sections first underwent the same sodium borohydride, cryoprotectant and freeze-thawing treatments as described in the pre-embedding immunoperoxidase EM immunocytochemistry section. They were then submerged in a pre-incubation solution for 60 minutes at RT and then washed multiple times in TBS-Gelatin (0.24g TRIS, 0.88g NaCl, 100µL Fish Gelatin, 100mL of Distilled Water, pH 7.6). This was followed by a pre-incubation in a PBS solution that contained 5% non-fat dry milk for 30 minutes at RT. Sections were then immersed in the GluD1 primary antibody solution containing TBS-Gelatin and 1% non-fat dry milk for 24 hours at RT, which was followed by thorough washes in TBS-Gelatin and a 2-hour incubation at RT in a gold-conjugated goat anti-rabbit secondary antibody (Cat#2004; Frontiers; 1:100) solution containing 1% non-fat dry milk and 98% TBS Gelatin. After rinses in TBS-Gelatin, sections were transferred to a 2% aqueous Acetate buffer solution (pH 7.0) before being processed with a HQ silver developing kit (Nanoprobes Inc., Yaphank, NY, USA) inside a dark room for 7-10 minutes. The reaction was stopped by repeated washes in acetate buffer. Sections were then gradually transferred to a phosphate buffer solution (PB, 0.05M, pH 7.4) by stepwise substitution of acetate buffer with PB. They were then post-fixed with osmium, dehydrated and embedded in resin, as described for the immunoperoxidase-stained sections, except that 0.5% osmium solution was used for 10 minutes and the 70% alcohol/uranyl acetate treatment was reduced to 10 minutes.

2.4 Light Microscopy Image Analysis

Six pairs of serially cut sections from the pre-commissural striatum of monkey MR-272L immunostained for either GluD1 or calbindin were digitally scanned by an Aperio ScanScope CS system (Aperio Technologies, Vista, CA) and analyzed using ImageScope software (Aperio Technologies). The pattern of GluD1 and calbindin labeling in the caudate nucleus from these

pairs of sections was assessed and qualitatively compared to determine the relationships between GluD1-enriched striatal regions with striosomes defined by their lack of calbindin immunostaining. Using the same approach, three pairs of sections through the pre-commissural striatum of the mouse RM-119 were immunostained for either GluD1 or MOR. From this material, the distribution pattern of striatal regions with low GluD1 expression was qualitatively compared with the localization of striosomes identified by strong MOR staining.

2.5 Electron Microscopy Image Analysis

Immunoperoxidase-stained Tissue

All tissue sections were examined under a JEOL JEM 1011 transmission electron microscope and images were acquired using an Erlagshen ES1000W Gatan Camera. Based on our light microscopic data indicating a differential level of GluD1 expression in the striosome and matrix striatal compartments (Fig. 1A-B) in mice and monkeys, blocks of tissue for EM analysis were chosen from either the striosome or the matrix compartment of the monkey caudate nucleus or only from the matrix compartment in mice. The delineation of striosomes and matrix from the GluD1-immunostained sections was based on adjacent sections stained for calbindin (for monkey) or MOR (for mice).

In the electron microscope, 50-60 micrographs of randomly distributed GluD1-immunostained elements were taken at 25,000X from both the striosomes and the matrix compartments of the caudate nucleus in each monkey or from the matrix compartment only in the pre-commissural dorsal striatum of mice. From these images, analyzed with the Gatan Digital Micrograph software, GluD1-labeled elements were counted and categorized as spine, dendrite, glia, axon or terminal based on their ultrastructural features (Peters et al. 1991). The mean

percentages of each category of GluD1-labeled profiles was then calculated by dividing the total number of specific labeled neuronal or glial structures by the total number of GluD1-labeled elements in each striatal compartment.

Immunogold-stained Tissue

In the immunogold-stained tissue, neuronal structures had to contain a minimum of three immunogold particles to be categorized as GluD1-immunoreactive, while a single gold particle was considered sufficient to categorize glial processes as GluD1-immunoreactive because of their small size. A total of 16-18 images of randomly distributed GluD1-labeled structures were taken at 25,000X-40,000X from the striatum of 3 mice and one monkey to corroborate the GluD1 localization seen in the immunoperoxidase-stained material. Due to the small sample size, only a qualitative description of the immunogold labeling is presented in this study.

2.6 Statistical Analysis

Inter-individual differences in the relative percentages of GluD1-positive elements between animals of the same group (mouse vs monkey and striosome vs matrix) were tested using one-way ANOVA in Sigmaplot 14.0 software. All data are presented as an average percentage value ± Standard Error of the Mean (SEM). Error bars account for variance between animals for each region of interest. Mice and monkey data were compared using two-sample t-tests to verify if there were any statistically significant species difference in the distribution of GluD1.

3. Results:

3.1 GluD1 is Differentially Expressed in the Striosome and Matrix Compartments of Mice vs Monkeys

In this first series of experiments, the overall distribution of striatal GluD1 immunoreactivity was analyzed from immunoperoxidase-stained tissue in mice and monkeys. As depicted in Figure 1, the pattern of striatal GluD1 immunostaining was heterogeneous in the dorsal striatum of both species. In the monkey caudate nucleus, small areas of strong GluD1 immunolabeling lay within a diffuse, less intensely stained, neuropil (Fig. 1A), a pattern reminiscent of the striosome/matrix striatal compartmentation (Graybiel 1990). Thus, to determine if the GluD1-enriched areas corresponded to the striosome striatal compartment, we compared the distribution of GluD1 with that of calbindin immunostaining in adjacent sections. As depicted in Figure 1A-B, there was a complete registration between dense GluD1-immunostained regions and calbindin-negative striosomes (Gerfen, 1985, Graybiel, 1990, Cote et al. 1991) in the pre-commissural striatum, thereby indicating that GluD1 immunoreactivity is differentially expressed between the striosomes and extrastriosomal matrix of the primate striatum.

Although the pattern of GluD1 immunostaining was also heterogeneous in the mouse striatum, the relationship with the striosome and matrix compartments was opposite to that shown in monkeys (Fig. 1C,D). As shown in Figure 1C, the mouse dorsal striatum neuropil was enriched in GluD1 immunostaining, except for small pockets of low immunoreactivity. When compared with adjacent sections immunostained for MOR, a commonly used marker of striosomes in rodents (Herkenham and Pert, 1981; Graybiel, 1990), the areas of low GluD1 immunoreactivity were in register with the striatal areas enriched in MOR, thereby suggesting that the striosome

compartment displays a lower level of GluD1 immunoreactivity than the matrix compartment in the precommissural mouse striatum (Fig. 1C-D).

3.2 Immunoperoxidase Localization of GluD1 in the Mouse and Monkey Striatum

Our next set of experiments aimed at assessing the subcellular localization of GluD1 in the mouse and monkey dorsal striatum using quantitative electron microscopy analysis of immunoperoxidase-stained tissue. Based on our light microscopy data, we sought to compare the ultrastructural localization of GluD1 in the striosome and matrix compartments of the monkey striatum to determine if the higher level of striosomal GluD1 immunoreactivity depicted in Fig 1A was related to any differences in the ultrastructural localization of GluD1 between the two striatal compartments. As stated above, this analysis was performed on tissue from the pre-commissural caudate nucleus, where the striosomes are more clearly delineated from the matrix. In mice, our EM analysis was focused on matrix tissue from the pre-commissural dorsal striatum, because the striosomes expressed very low levels of GluD1 immunoreactivity.

The pattern of GluD1 immunoreactivity seen within specific neuronal elements was largely the same between striosome vs matrix regions and across animal species (Figs 2-3). Within dendritic shafts, dense peroxidase staining, that occasionally diffused into the synaptic cleft, was often aggregated at the post-synaptic densities (PSD) of asymmetric synapses (Fig. 3C-D). We also encountered dendritic profiles with dense GuD1 staining along the plasma membrane at sites devoid of clear synaptic contacts (Fig. 3A). In other instances, the peroxidase deposit was intracellular adjacent to the external membrane of mitochondria (Fig 2. A-C; Fig. 3A,E). In labeled spines, the extent of GluD1 immunoreactivity was variable, ranging from nearly completely filled spine heads and necks (Fig. 2D) to restricted staining associated with the PSD of asymmetric axo-

spinous synapses (Fig. 3A). GluD1-immunoreactive unmyelinated axonal profiles, which were only found in the monkey striatum, were identified as darkly stained circular structures with microtubules surrounded by other unlabeled axons (Fig. 3E). Although rare, GluD1-positive terminals with light plasma membrane staining were occasionally seen within the monkey caudate. Glial GluD1-immunostained processes were sometimes located near GluD1-labeled synapses (Fig. 2C; Fig. 3A,C) or in the striatal neuropil without any obvious associations with specific neuronal elements (Fig. 2A-B; Fig. 3B).

Inter-individual differences in the relative distribution of GluD1 between animals of the same group (striosome vs matrix) were tested using one-way ANOVA. Based on this analysis, which did not reveal any significant within-group differences, quantitative data reported in figure 5 are average percentages ± SEM of pooled data from 3 mice and 3 monkeys per group. Overall, the present findings confirm and extend data from our recent study (Liu et al. 2020). In brief, GluD1 immunoreactivity in the mouse dorsal striatum was preferentially associated with dendritic shafts (47.9 ± 1.2% of total labeled structures) and glia (37.7 ± 2.5%), but significantly less abundant in dendritic spines (14.3 ± 2.6%) (Fig. 5A). A comparable trend was found in both the striosome and matrix compartments within the pre-commissural caudate nucleus in monkeys. In the striosome compartments, GluD1 was also preferentially found in dendritic shafts (44.4 ± 2.8% of total labeled elements) and glia (36.4 ± 0.4%) compared to spines (12.5 ± 2.7%), axon terminals (1.8 ± 0.3%) and unmyelinated axons (4.8 ± 7.2%) (Fig. 5B). Overall, the pattern was the same in the matrix, ie dendritic shafts accounted for the largest proportion of GluD1-labeled structures (49.0 ± 1.5%) followed by glia (33.8 ± 3.9%), spines (12.7 ± 1.5%), axons (7.2 ± 1.5%) and axon terminals (1.2 ± 0.3%) (Fig. 5B). A two-sample t-test analysis of the relative proportion of GluD1-labeled elements between the striosome and matrix compartments of the pre-commissural monkey

caudate did not reveal any significant difference between the two compartments (dendrites p=0.870; glia p=0.548; spines p=0.953; axons p=0.243; terminals p=0.268). A two-sample t-test comparing the relative proportion of GluD-1 labeled elements between the matrix compartments of mice and monkeys also yielded no statistically significant differences (dendrites p=0.140; glia p=0.451; spines p=0.633).

3.3 Immunogold Localization of GluD1 in the Mouse Striatum

In a third set of experiments, we sought to further enhance our knowledge of the subcellular (and subsynaptic) localization of GluD1 in the mouse and monkey striatum using the pre-embedding immunogold approach. However, due to technical challenges in using the GluD1 antibodies to reliably assess the localization of GluD1 with gold particles in many of our animals, results reported in this part of study were collected from the striatal tissue of one monkey (MR-272L) and three mice (RM-12, RM-74, RM-76). A lower cut-off of three or more immunogold particles per neuronal elements was arbitrarily set to differentiate immunoreactive from non-immunoreactive neuronal elements, while in glia, a single gold particle was considered as an evidence of GluD1 immunoreactivity because of their small size. Due to the low number of animals that could be used in these experiments, statistical analyzes were not performed.

As depicted in figure 4, both plasma membrane-bound and intracellular gold particles were found in GluD1-positive dendrites and spines. In some instances, the plasma membrane-bound gold labeling was aggregated at the edges of the PSDs of asymmetric synapses (Fig. 4A-B) or located at non-synaptic sites along the plasma membrane (Fig. 4A), while the intracellular labeling was commonly seen in close apposition with the membrane of mitochondria or attached to microtubules (Fig. 4C). Because of their small diameter relative to the size of the silver-intensified

gold particles, glial processes contained GluD1 gold labeling that filled the whole processes without any clear distinction between the plasma membrane-bound vs intracellular compartment (Fig. 4B).

4. Discussion:

Our findings reveal that GluD1 is differentially expressed in the striosome and matrix compartments of the mouse and monkey striatum. Such a finding is surprising, since the striatum is often considered a region of conserved anatomy and function within mammals (Herkenham and Perf. 1981; Friedman et al. 2015). At the electron microscopic level, our ultrastructural analysis revealed that GluD1 is preferentially expressed in dendritic shafts, followed by glia, and then dendritic spines. This pattern remained consistent in both the striosome and matrix compartments of the pre-commissural caudate nucleus in monkeys, as well as for the dorsal striatal matrix of the mouse. In addition, the monkey caudate also contained a small number of GluD1-immunoreactive unmyelinated axons and axon terminals that were not present in the mouse. The overall similarity in the ultrastructural localization of GluD1 expression between the striosome and matrix compartments of mice and monkey striatum suggest that GluD1 may mediate its effects in the dorsal striatum through regulation of common neuronal and glial targets. A qualitative subcellular and subsynaptic localization of GluD1 confirmed its presence within glial processes, and also demonstrated that GluD1 distributes itself nearby putative glutamatergic axo-dendritic and axo-spinous synapses and at non-synaptic sites along the plasma membrane as well as along the external membrane of mitochondria in the intracellular compartment.

4.1 GluD1's Consistent Distribution in Neuronal Elements Suggests a Common Function for the Receptor Channel

We reported that GluD1's prevalence in the monkey striatum at the LM level differed along the striosome vs matrix axis, with striosomes containing higher amounts of immunoreactivity, while the opposite was true in mice, such that the matrix was more enriched in GluD1

immunoreactivity than the striosomes. This finding is of particular note, since the striosomes and surrounding matrix have significantly different afferent and efferent connections and display distinct neurochemical environments, suggesting differential functions between the two regions (Graybiel and Ragsdale. 1978; Roberts et al. 2002; Roberts et al. 2005). For example, the Parafascicular (Pf) nucleus of the thalamus selectively innervates the striatal matrix compartment, while the striosomes contain afferents from other areas such as the midline thalamic nuclei (Sadikot et al. 1990; Ragsdale and Graybiel. 1991; Unzai et al. 1991; Smith et al. 2014). Moreover, striatal projection neurons in the striosomes are a major source of GABAergic inputs to the dopaminergic neurons of the substantia nigra compacta (SNc), while striatal neurons in the matrix project to the substantia nigra pars reticulate and the globus pallidus (Crittenden and Graybiel. 2011; Fujiyama et al. 2011).

The striosome/matrix compartmentation, however, is generally conserved across species like other regions of the basal ganglia (Herkenham and Perf. 1981; Friedman et al. 2015). At first glance, the differential striosomal expression of GluD1 between mice and monkeys reported in our study suggest that GluD1 could be playing a different species-specific role in the matrix relative to the striosome compartments between mice and monkeys. However, because there was no major difference in the pattern of GluD1 immunoreactivity between different neuronal and glial elements in the striosome vs matrix compartments of the monkey caudate or between monkeys and mice at the electron microscopic level, the potential functional differences of GluD1 between the two species or compartments cannot be explained by a change in the proportional distribution of GluD1 among neuronal and glial structures alone. Instead, it may be possible that GluD1 is performing a similar function between the striosome and matrix compartments by interacting with afferents to the striatum that are each unique among the striosome and matrix and which differ between

monkeys and mice. While we found some GluD1 immunoreactivity within axons and axon terminals in the pre-commissural monkey caudate nucleus, but not in the mouse striatum, the functional significance of this rather scarce pre-synaptic labeling remains unclear.

4.2 GluD1 Interactions with Thalamostriatal Afferents: A Potential Role of Cerebellin and More in Primates?

As noted earlier, GluD1 works in concert with presynaptic Cerebellin (Cbln) and Neurexin (Nxn) to help physically anchor presynaptic and postsynaptic components of specific glutamatergic synapses (Uemura et al. 2010; Yuzaki. 2018; Nakamoto et al. 2020). As its name implies, Cbln1 originates from, and is most prolific in, the cerebellum (Ibata et a. 2019). Among the various sources of striatal afferents, Cbln1 is abundant in the Pf nucleus of the thalamus, which is known as the main origin of the thalamostriatal system that selectively innervates the matrix of the striatum (Herkenham and Pert. 1981; Kusnoor et al. 2009; Kusnoor et al. 2010; Smith et al. 2014). This aligns with what we have observed from GluD1's immunoperoxidase reactivity in the mouse striatum (Fig. 1C), such that the matrix compartment contains relatively high levels of peroxidase staining, while the striosomes display very little, if any, staining. However, the situation is different in primates, since the striosomes of the monkey caudate nucleus show a greater level of immunoreactivity relative to the matrix (Fig. 1A). Because the Pf also projects exclusively to the striatal matrix compartment in monkeys (Smith et al. 2014), our findings suggest that GluD1 may interact with a different source of striatal afferents and/or different presynaptic partner in the striosomes.

GluD1 does bind to other presynaptic Cbln proteins, such as Cbln2. The stronger striosomal expression of GluD1 in the pre-commissural monkey caudate nucleus could potentially indicate

GluD1's interaction with Cbln coming from other limbic nuclei. The striosomes have long been thought as the striatum's center of communication with the limbic cortices (Miyamoto et al. 2018). Given GluD1 mRNA localization in the rodent brain, some potential sources of Cbln1 to the striosome compartments could be limbic cortices or non-Pf anterior thalamic nuclei. However, this remains highly speculative without a detailed analysis of the striatal projections of Cbln1-containing cortical and thalamic neurons, and the lack of Cbln1 localization in the monkey brain. Another potential partner of GluD1 in the striosomes could be Cerebellin-2 (Cbln2) which displays a far more widespread distribution than Cbln1 at the cortical and subcortical level, including regions known to innervate striosomes (limbic cortex, midline thalamic nuclei, etc.) (Allen Brain Atlas). However, GluD1 shows a stronger preference for Cbln1 over Cbln2 (Wei et al. 2012), which reduces the likelihood that Cbln2 may be the key partner of GluD1 in striosomes, although such interactions must be directly tested. GluD1's interaction with other presynaptic proteins, while not described, is plausible. GluD2's role in the cerebellum and the focus on specific viral tracing from the cerebellum for GluD1 could have resulted in other sources of GluD1 or its interacting proteins being potentially overlooked. Further investigations will be needed in the striosomes of the precommissural monkey caudate to ascertain precisely with what GluD1 is interacting with.

4.3 Potential GluD1 Expression in Mitochondria and Glia

Both our immunoperoxidase and immunogold labeling demonstrated extrasynaptic and intracellular GluD1expression near mitochondrial membranes in dendritic shafts. To date, there is no literature regarding GluD1 functions in mitochondria. However, preliminary mass spectroscopy data from the mitochondria of GluD1-positive neuronal elements appear to show the presence of

GluD1-associated proteins, potentially shedding light onto why GluD1 can be found apposed outer mitochondrial membranes (Shashank and colleagues – personal communication).

Our immunoperoxidase and immunogold data additionally showed that GluD1 is expressed in glial processes throughout the pre-commissural monkey caudate and the pre-commissural dorsal mouse striatum. At first, this finding appears to be incongruous with GluD1's preferential association with glutamatergic neurons. Yet, recent findings have shown that GluD1 mRNA is located in certain types of glia – specifically oligodendrocyte precursor cells (OPC) (Larson et al. 2016; Saunders et al. 2018). OPCs are glia that often differentiate into myelinating oligodendrocytes throughout the brain (Antel et al. 2018; Berry et al. 2020), but this is not their only function. Many do not become oligodendrocytes and instead can form synapses with diverse subgroups of neurons, including with glutamatergic afferents (Bergles et al. 2000; Ziskin et al 2007; Bergles et al. 2010). The precise purpose of these synaptic formations remains largely unknown, but they are speculated to be either part of the OPC differentiation process or otherwise involved in an unidentified function (Kukley et al. 2010; Hill and Nishiyama. 2014). The presence of GluD1 within these cells could have to do with a differentiation process, since GluD1 helps to form mature synapses in developing neuropil (Gupta et al. 2015; Hepp et al. 2015). However, GluD1 also maintains glutamatergic synapses in the adult mammalian brain (Konno et al. 2014; Suryavanshi et al. 2016). Therefore, its presence in OPCs could signify meaningful long-term glutamatergic activity.

4.4 Future Directions:

As previously noted, the goal of this study was to provide a detailed map of the regional, cellular and subcellular localization of GluD1 in the mouse and monkey striatum. Our findings of

a differential expression of GluD1 immunoreactivity in the striosomes and matrix between mice and monkeys are intriguing and necessitate further studies. While it is likely that the darker GluD1 staining in the monkey striosomes over the matrix is representative of an increase in the number of immunostained elements, a density analysis of GluD1's immunoperoxidase expressing elements within each region (striosome vs matrix) of both mice and monkeys would help directly address this issue. Furthermore, knowing the density of GluD1-positive profiles within the striosome and matrix of the monkey striatum would allow for a more reliable comparison with data from the matrix of the mouse striatum.

Confirmation of GluD1's synaptic partners within the striosomes of the monkey caudate is another necessary next step from the work we have shown. One method to accomplish this would likely be a pairing of GluD1 immunogold labeling with immunoperoxidase staining for pre-synaptic Cbln1 and Cbln2 for use at the EM level. Such double immunolabeling assays are well established means of establishing a link between pre- and postsynaptic partners (Niranberg et al. 1997; Chan et al. 2010; Galvan et al. 2016). Thus, by labeling GluD1 – the postsynaptic partner – with immunogold, and Cbln1/2 – the presynaptic partner – with immunoperoxidase, we will be able to determine the frequency of co-expression of the two proteins at individual synapses. If GluD1 immunogold particles are associated with pre-synaptic terminals that do not express Cbln1 or Cbln2, it will suggest that some of the striatal GluD1 may interact with other pre-synaptic partners than Cbln1 and Cbln2. In this case, molecular analyses such as isolating GluD1-active synaptosomes and using mass spectroscopy could potentially be used to ascertain GluD1's unidentified presynaptic target protein (Villasana et al. 2006).

Double immunolabeling could additionally be useful to further characterize GluD1 expression in glial cells. The most likely candidate for glial GluD1 expression is the OPC, yet

definitive confirmation of the receptor expression in this cell type has not been demonstrated. Labeling GluD1 with immunogold and OPCs with immunoperoxidase would allow for direct confirmation of GluD1 expression in OPCs or otherwise reveal its presence in other glial cells such as astrocytes. Such data will help set the stage for further functional studies of GluD1 in glia.

Determining whether the glutamatergic terminals making contact with postsynaptic striatal GluD1-positive elements are primarily from the thalamus or the cortex in rodents and monkeys is further crucial step from the data that we have shown. This could once again be accomplished using double immunolabeling. Presynaptic vesicular glutamate transporters (vGluT) 1-2 are very specific in their expression within the striatum. vGluT1 is a specific marker for cortical afferents leading to the striatum, while vGluT2 mediates thalamic inputs to the striatum. Furthermore, it has been demonstrated by Liu et al. that striatal GluD1 KO does affect vGluT2 expression at the confocal microscopic level (Raju et al. 2008; Smith et al. 2014; Liu et al. 2020). Therefore, by labeling GluD1 with immunogold and vGluT1/2 with immunoperoxidase, the precise interaction of GluD1 with either the corticostriatal or thalamostriatal system could be confirmed. Additionally, such an experiment would demonstrate how GluD1 localizes itself at the subsynaptic level in relation to such terminals.

Tables and Figures:

Animal ID	Gender	Age	Analysis Type
MR-271L	Male	2 years 9 months	EM
MR-272L	Male	3 years 3 months	LM/EM
MR-292L	Male	2 years 6 months	EM

Table 1: Relevant data on monkeys used in the experiment

Animal ID	Gender	Genetic Line	Age	Analysis Type
RM-12	Male	No genetic mutation	45 days	EM
RM-74	Male	RGS9 Cre+ GluD1 flox -/-	22 days	EM
RM-75	Male	RGS9 Cre+ GluD1 flox -/-	20 days	EM
RM-76	Male	RGS9 Cre+ GluD1 flox -/-	20 days	EM
RM-119	Male	No genetic mutation	79 days	LM

Table 2: Relevant data on mice used in the experiment

Antibody Name	Species	Vender	Dilution	References
GluD1C-Af1390	Rabbit	Frontier Institute Company Ltd	1:5000	Liu et al. 2020
Calbindin D-28R-C9848	Mouse	Sigma Aldrich Company Ltd	1:4000	Gerfen et al. 1985
Mu-Opiod Receptor-Ab1580 (MOR)	Rabbit	Millipore Sigma Company Ltd	1:10000	Herkenham and Pert. 1981

Table 3: Specific antibody information

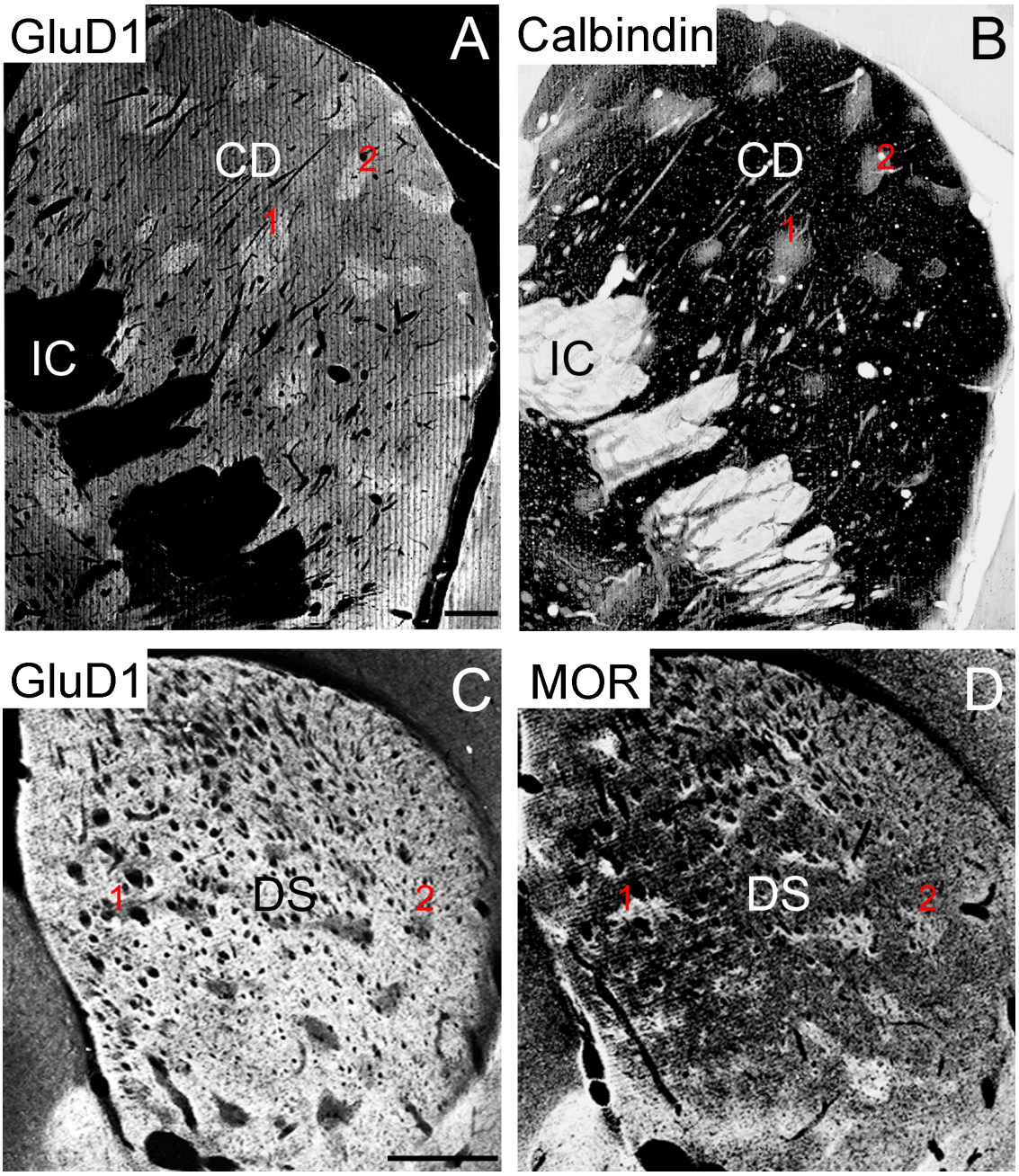

Figure 1(A-D): Striosome/Matrix Compartmentation of GluD1 in the monkey and mouse striatum. Light micrographs of GluD1 immunoperoxidase staining in the pre-commissural caudate nucleus of a monkey (A) and the pre-commissural dorsal striatum of a mouse (C). (B) and (D) illustrate adjacent sections immunostained for calbindin D28k (B) or MOR (D) to differentiate the striosomes from the matrix compartments of the monkey and mouse striatum, respectively. Note the close correspondence between dense patches of GluD1 immunostaining in A with calbindin-immunonegative striosomes in B. In mouse, areas of low GluD1 labeling in C correspond to MOR-enriched striosomes in D (red-colored numbers). Note that colors in panels A, C and D have been inverted, i.e. low intensity coloring indicates higher levels of GluD1 immunoreactivity. Abbreviations: CD: caudate nucleus, DS: dorsal striatum, IC: internal capsule. Scale bar in A (applies to B) = 1 mm. Scale bar in C (applies to D) = 0.5 mm.

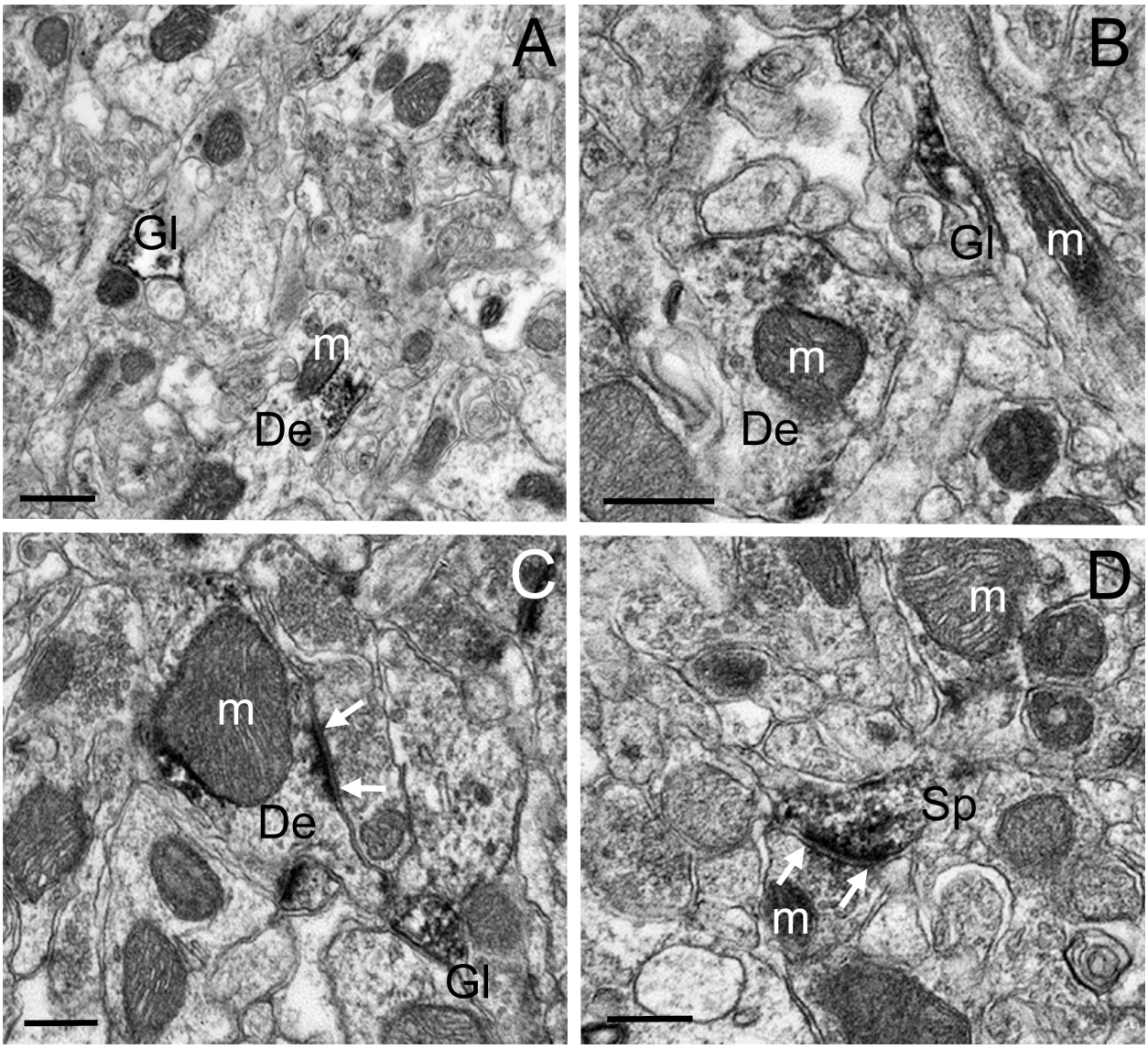

Figure 2 (A-D): GluD1-immunoreactive elements in the mouse striatum. Examples of different GluD1-immunoreactive dendrites (A-C), spines (D) and glia (A,B) in the mouse dorsal striatum. In C and D, white arrows indicate an asymmetric axo-dendritic (C) and an axo-spinous (D) synapse. Note some GluD1 labeling apposed to the surface of mitochondria in A-C. Abbreviations: Spine (Sp), Dendrite (De), Glia (Gl) and Mitochondria (m). Scale bar in A = 0.50µm. Scale bar in B = 0.35µm. Scale bar in C = 0.25µm. Scale bar in D = 0.25µm.

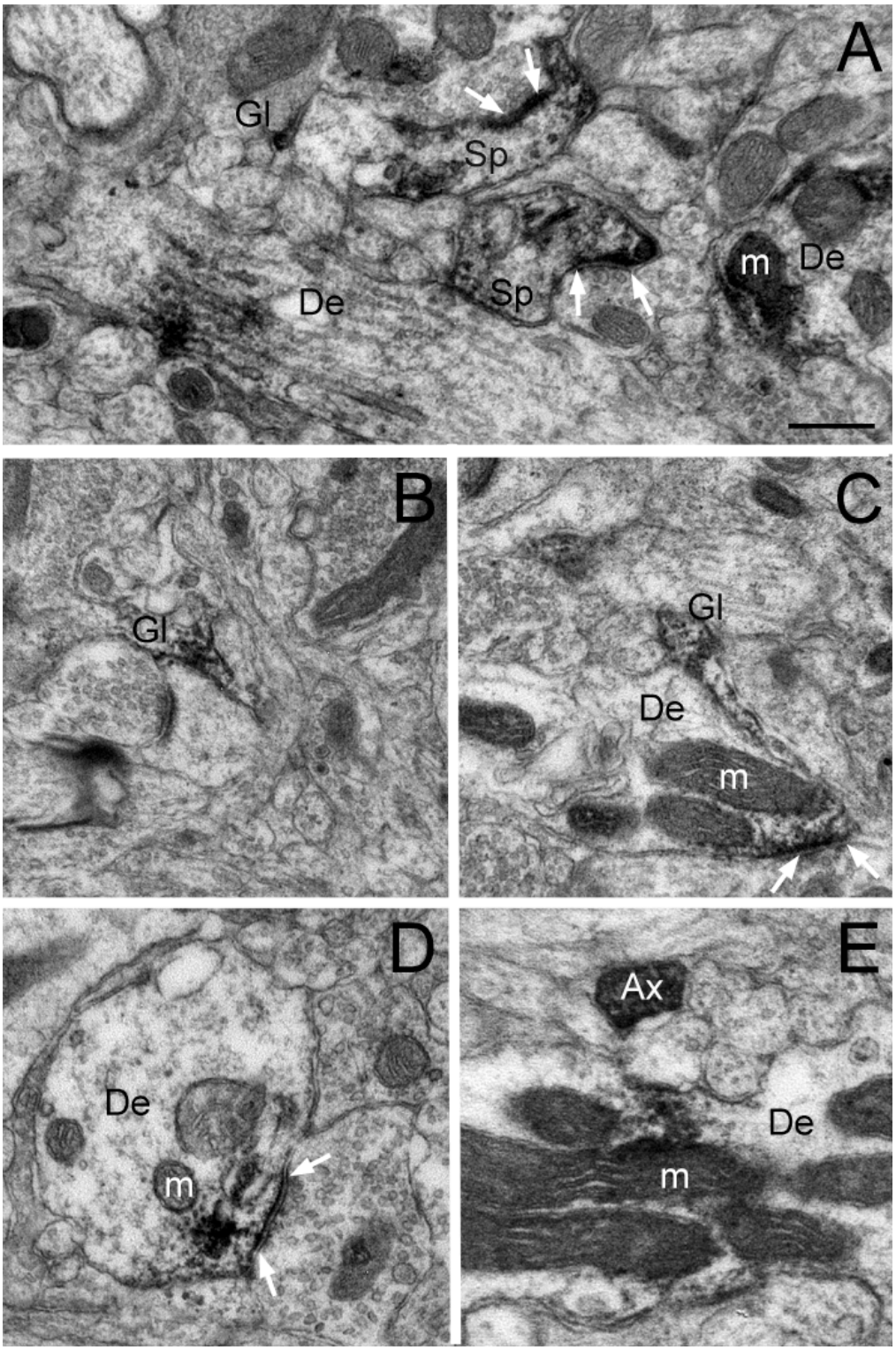

Figure 3 (A-E): GluD1-immunoreactive elements in the monkey striatum. Examples of different GluD1-positive neuronal and glial structures in the monkey striatum. White arrows indicate asymmetric synapses with dense aggregates of GluD1 imunolabeling in their close vicinity. Abbreviations: Spine (Sp), Dendrite (De), Glia (Gl), unmyelinated axon (Ax) and Mitochondria (m). Scale bar in A (applies to B-E) = 0.30μm.

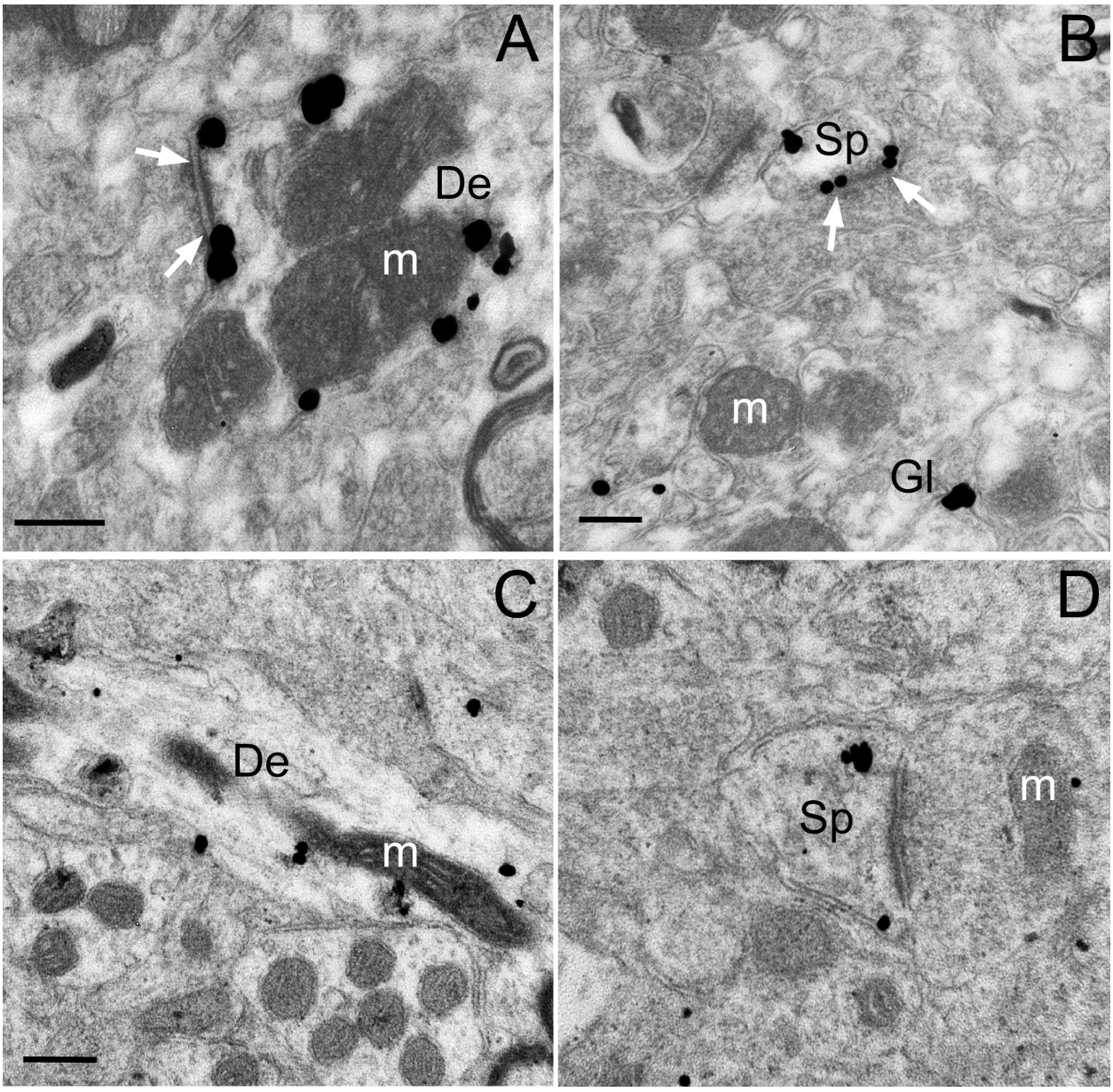

Figure 4 (A-D): Immunogold localization of GluD1 in the mouse and monkey striatum. Examples of GluD1-immunoreactive dendrites and spines in the mouse (A,B) and monkey (C,D) striatum as revealed with the pre-embedding immunogold technique. White arrows indicate asymmetric synapses that display GluD1 immunoreactivity within the neuronal element. Abbreviations: Spine (Sp), Dendrite (De), Glia (Gl) and Mitochondria (m). Scale bar in A = 0.25µm. Scale bar in B = 0.22µm. Scale bar in C (applies to D) = 0.25µm.

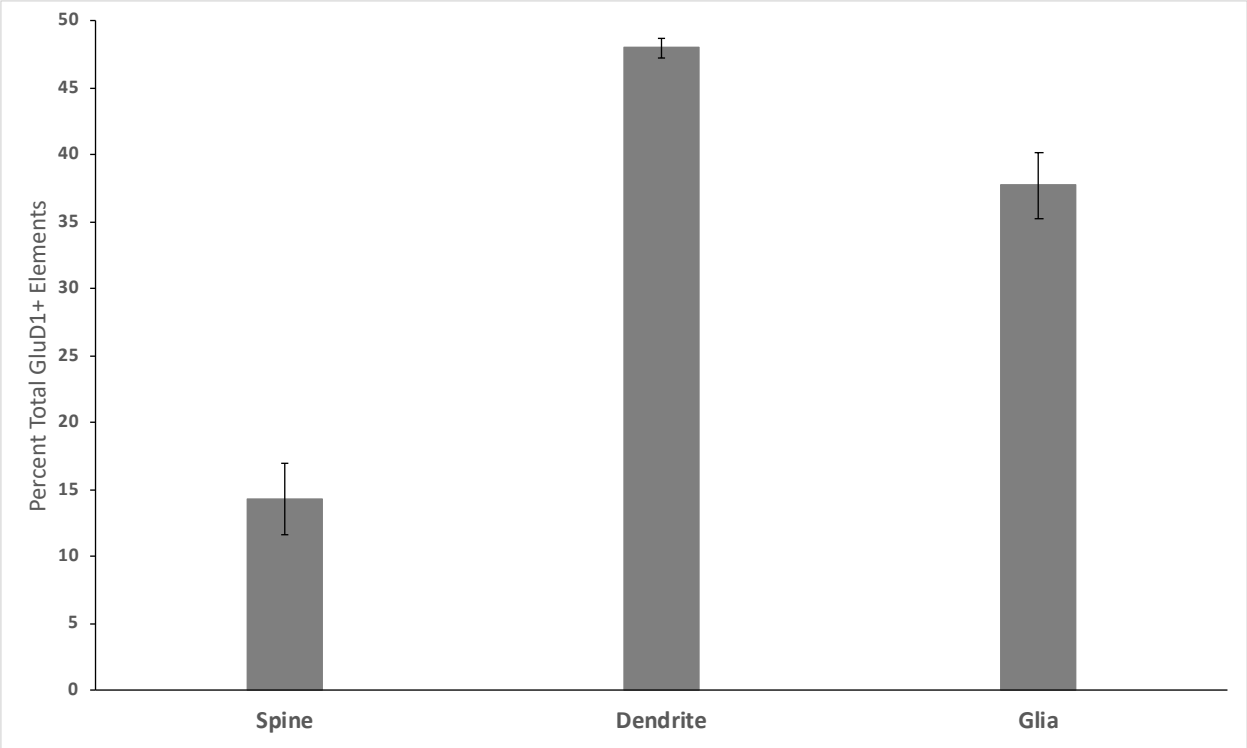

Figure 5: *Relative Distribution of GluD1-immunostained elements in the Precommissural Dorsal Mouse Striatum*. This figure shows the mean relative percentages (+/- SEM) of GluD1-positive neuronal and glial structures in the matrix compartment of the mouse dorsal striatum (N=3 animals; n=324 images). There is also no statistically significant difference between the percentages of GluD1-immunoreactive elements of the mouse vs the monkey matrix compartment (two-sample t-test; dendrites p=0.140; glia p=0.451; spines p=0.633).

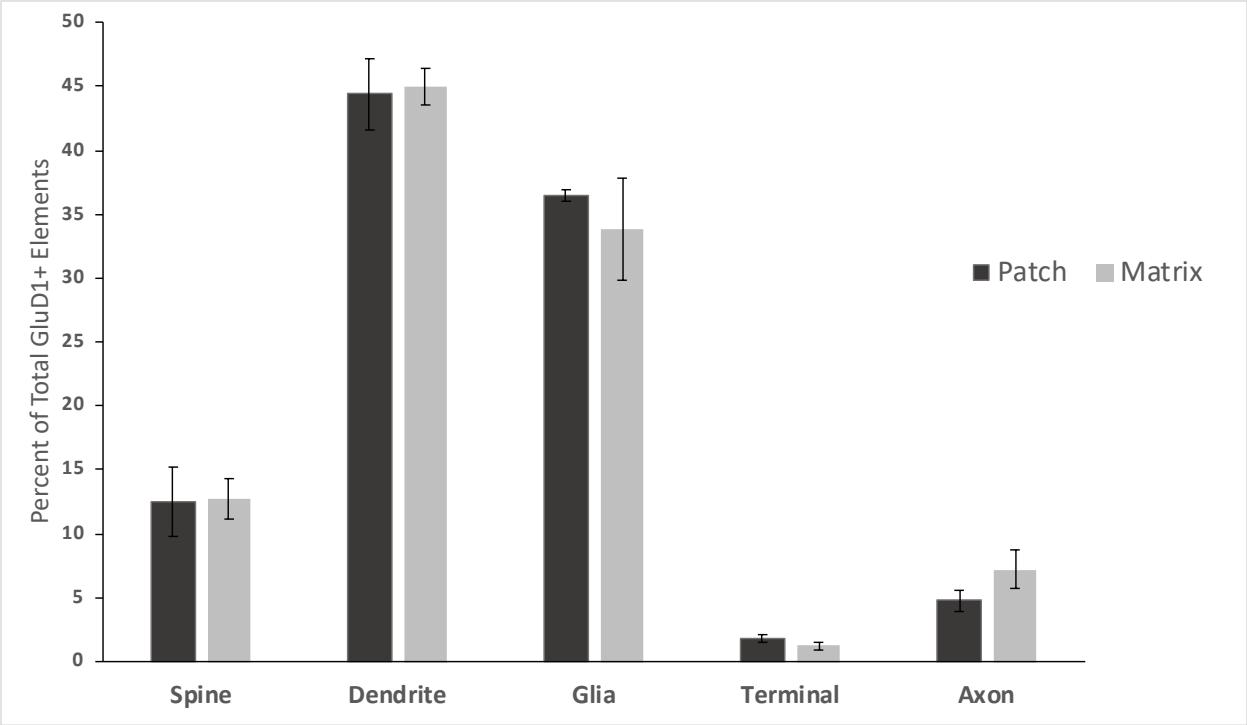

Figure 6: *Relative Distribution of GluD1-immunostained elements*. This graph illustrates the relative percentage of GluD1-immunostained elements in the striosome vs matrix compartments of the monkey caudate nucleus (N=3 animals; n=157 images). There is no statistically significant difference in the relative percentages of the different neuronal and glial elements between the striosome and matrix compartments (two sample t-test; dendrites p=0.870; glia p=0.548; spines p=0.953; axons p=0.243; terminals p=0.268). There is also no statistically significant difference between the percentages of GluD1-immunoreactive elements of the mouse vs the monkey matrix compartment (two-sample t-test; dendrites p=0.140; glia p=0.451; spines p=0.633).

References:

Antel, J. P., Lin, Y. H., Cui, Q.-L., Pernin, F., Kennedy, T. E., Ludwin, S. K., & Healy, L. M. (2019). Immunology of oligodendrocyte precursor cells in vivo and in vitro. *Journal of Neuroimmunology*, *331*, 28–35. https://doi.org/10.1016/j.jneuroim.2018.03.006

Benamer, N., Marti, F., Lujan, R., Hepp, R., Aubier, T. G., Dupin, A. a. M., Frébourg, G., Pons, S., Maskos, U., Faure, P., Hay, Y. A., Lambolez, B., & Tricoire, L. (2018). GluD1, linked to schizophrenia, controls the burst firing of dopamine neurons. *Molecular Psychiatry*, *23*(3), 691–700. https://doi.org/10.1038/mp.2017.137

Bergles, D. E., Jabs, R., & Steinhäuser, C. (2010). Neuron-glia synapses in the brain. *Brain Research Reviews*, *63*(1–2), 130–137. https://doi.org/10.1016/j.brainresrev.2009.12.003

Bergles, D. E., Roberts, J. D. B., Somogyi, P., & Jahr, C. E. (2000). Glutamatergic synapses on oligodendrocyte precursor cells in the hippocampus. *Nature*, *405*(6783), 187–191. https://doi.org/10.1038/35012083

Berridge, G., Menassa, D. A., Moloney, T., Waters, P. J., Welding, I., Thomsen, S., Zuberi, S., Fischer, R., Aricescu, A. R., Pike, M., Dale, R. C., Kessler, B., Vincent, A., Lim, M., Irani, S. R., & Lang, B. (2018). Glutamate receptor δ2 serum antibodies in pediatric opsoclonus myoclonus ataxia syndrome. *Neurology*, *91*(8), e714–e723. https://doi.org/10.1212/WNL.0000000000006035

Berry, K., Wang, J., & Lu, Q. R. (2020). Epigenetic regulation of oligodendrocyte myelination in developmental disorders and neurodegenerative diseases. *F1000Research*, *9*. https://doi.org/10.12688/f1000research.20904.1

Brimblecombe, K. R., & Cragg, S. J. (2017). The Striosome and Matrix Compartments of the Striatum: A Path through the Labyrinth from Neurochemistry toward Function. *ACS Chemical Neuroscience*, *8*(2), 235–242. https://doi.org/10.1021/acschemneuro.6b00333

Chan, J., Aoki, C., & Pickel, V. M. (1990). Optimization of differential immunogold-silver and peroxidase labeling with maintenance of ultrastructure in brain sections before plastic embedding. *Journal of Neuroscience Methods*, *33*(2–3), 113–127.

Côté, P.-Y., Sadikot, A. F., & Parent, A. (1991). Complementary Distribution of Calbindin D-28k and Parvalbumin in the Basal Forebrain and Midbrain of the Squirrel Monkey. *European Journal of Neuroscience*, *3*(12), 1316–1329. https://doi.org/10.1111/j.1460-9568.1991.tb00064.x

Crittenden, J. R., & Graybiel, A. M. (2011). Basal Ganglia Disorders Associated with Imbalances in the Striatal Striosome and Matrix Compartments. *Frontiers in Neuroanatomy*, *5*. https://doi.org/10.3389/fnana.2011.00059

Electrophysiological properties of NG2+ cells: Matching physiological studies with gene expression profiles. (n.d.). Retrieved April 5, 2020, from https://www.ncbi.nlm.nih.gov/pmc/articles/PMC4792778/

Flaherty, A. W., & Graybiel, A. M. (1994). Input-output organization of the sensorimotor striatum in the squirrel monkey. *The Journal of Neuroscience: The Official Journal of the Society for Neuroscience*, *14*(2), 599–610.

Friedman, A., Homma, D., Gibb, L. G., Amemori, K., Rubin, S. J., Hood, A. S., Riad, M. H., & Graybiel, A. M. (2015). A Corticostriatal Path Targeting Striosomes Controls Decision-Making under Conflict. *Cell*, *161*(6), 1320–1333. https://doi.org/10.1016/j.cell.2015.04.049

Fujiyama, F., Sohn, J., Nakano, T., Furuta, T., Nakamura, K. C., Matsuda, W., & Kaneko, T. (2011). Exclusive and common targets of neostriatofugal projections of rat striosome neurons: A single neuron-tracing study using a viral vector. *The European Journal of Neuroscience*, *33*(4), 668–677. https://doi.org/10.1111/j.1460-9568.2010.07564.x

Galvan, A., Smith, Y., & Wichmann, T. (2016). Effects of Optogenetic Activation of Corticothalamic Terminals in the Motor Thalamus of Awake Monkeys. *The Journal of Neuroscience*, *36*(12), 3519–3530. https://doi.org/10.1523/JNEUROSCI.4363-15.2016

Gerfen, C. R., Baimbridge, K. G., & Miller, J. J. (1985). The neostriatal mosaic: Compartmental distribution of calcium-binding protein and parvalbumin in the basal ganglia of the rat and monkey. *Proceedings of the National Academy of Sciences of the United States of America*, *82*(24), 8780–8784.

Graybiel, A M, & Ragsdale, C. W. (1978). Histochemically distinct compartments in the striatum of human, monkeys, and cat demonstrated by acetylthiocholinesterase staining. *Proceedings of the National Academy of Sciences of the United States of America*, *75*(11), 5723–5726.

Graybiel, Ann M. (1990). Neurotransmitters and neuromodulators in the basal ganglia. *Trends in Neurosciences*, *13*(7), 244–254. https://doi.org/10.1016/0166-2236(90)90104-I

Gupta, S. C., Yadav, R., Pavuluri, R., Morley, B. J., Stairs, D. J., & Dravid, S. M. (2015). Essential role of GluD1 in dendritic spine development and GluN2B to GluN2A NMDAR subunit switch in the cortex and hippocampus reveals ability of GluN2B inhibition in correcting hyperconnectivity. *Neuropharmacology*, *93*, 274–284. https://doi.org/10.1016/j.neuropharm.2015.02.013

Hepp, R., Hay, Y. A., Aguado, C., Lujan, R., Dauphinot, L., Potier, M. C., Nomura, S., Poirel, O., El Mestikawy, S., Lambolez, B., & Tricoire, L. (2015). Glutamate receptors of the delta family are widely expressed in the adult brain. *Brain Structure & Function*, *220*(5), 2797–2815. https://doi.org/10.1007/s00429-014-0827-4

Herkenham, M., & Pert, C. B. (1981). Mosaic distribution of opiate receptors, parafascicular projections and acetylcholinesterase in rat striatum. *Nature*, *291*(5814), 415–418. https://doi.org/10.1038/291415a0

Hill, R. A., & Nishiyama, A. (2014). NG2 Cells (Polydendrocytes): Listeners to the Neural Network with Diverse Properties. *Glia*, *62*(8), 1195–1210. https://doi.org/10.1002/glia.22664
Hirano, T. (2012). Glutamate-receptor-like molecule GluRδ2 involved in synapse formation at parallel fiber-Purkinje neuron synapses. *Cerebellum (London, England)*, *11*(1), 71–77. https://doi.org/10.1007/s12311-010-0170-0

Ibata, K., Kono, M., Narumi, S., Motohashi, J., Kakegawa, W., Kohda, K., & Yuzaki, M. (2019). Activity-Dependent Secretion of Synaptic Organizer Cbln1 from Lysosomes in Granule Cell Axons. *Neuron*, *102*(6), 1184-1198.e10. https://doi.org/10.1016/j.neuron.2019.03.044

Ichikawa, R., Sakimura, K., & Watanabe, M. (2016). GluD2 Endows Parallel Fiber–Purkinje Cell Synapses with a High Regenerative Capacity. *Journal of Neuroscience*, *36*(17), 4846–4858. https://doi.org/10.1523/JNEUROSCI.0161-16.2016

Kakegawa, W., Kohda, K., & Yuzaki, M. (2007). The δ2 'ionotropic' glutamate receptor functions as a non-ionotropic receptor to control cerebellar synaptic plasticity. *The Journal of Physiology*, *584*(Pt 1), 89–96. https://doi.org/10.1113/jphysiol.2007.141291

Karki, S., Maksimainen, M. M., Lehtiö, L., & Kajander, T. (2019). Inhibitor screening assay for neurexin-LRRTM adhesion protein interaction involved in synaptic maintenance and neurological disorders. *Analytical Biochemistry*, *587*, 113463. https://doi.org/10.1016/j.ab.2019.113463

Konno, K., Matsuda, K., Nakamoto, C., Uchigashima, M., Miyazaki, T., Yamasaki, M., Sakimura, K., Yuzaki, M., & Watanabe, M. (2014). Enriched Expression of GluD1 in Higher Brain Regions and Its Involvement in Parallel Fiber–Interneuron Synapse Formation in the Cerebellum. *The Journal of Neuroscience*, *34*(22), 7412–7424. https://doi.org/10.1523/JNEUROSCI.0628-14.2014

Kukley, M., Nishiyama, A., & Dietrich, D. (2010). The Fate of Synaptic Input to NG2 Glial Cells: Neurons Specifically Downregulate Transmitter Release onto Differentiating Oligodendroglial Cells. *The Journal of Neuroscience*, *30*(24), 8320–8331. https://doi.org/10.1523/JNEUROSCI.0854-10.2010

Kusnoor, S. V., Parris, J., Muly, E. C., Morgan, J. I., & Deutch, A. Y. (2010). Extracerebellar role for Cerebellin1: Modulation of dendritic spine density and synapses in striatal medium spiny neurons. *The Journal of Comparative Neurology*, *518*(13), 2525–2537. https://doi.org/10.1002/cne.22350

Kusnoor, Sheila V., Muly, E. C., Morgan, J. I., & Deutch, A. Y. (2009). Is the loss of thalamostriatal neurons protective in parkinsonism? *Parkinsonism & Related Disorders*, *15*(Suppl 3), S162–S166. https://doi.org/10.1016/S1353-8020(09)70806-5

Larson, V. A., Zhang, Y., & Bergles, D. E. (2016). Electrophysiological properties of NG2+ cells: Matching physiological studies with gene expression profiles. *Brain Research*, *1638*(Pt B), 138–160. https://doi.org/10.1016/j.brainres.2015.09.010

Liu, J., Gandhi, P. J., Pavuluri, R., Shelkar, G. P., & Dravid, S. M. (2018). Glutamate delta-1 receptor regulates cocaine-induced plasticity in the nucleus accumbens. *Translational Psychiatry*, *8*(1), 1–10. https://doi.org/10.1038/s41398-018-0273-9

Liu, J., Shelkar, G. P., Gandhi, P. J., Gawande, D. Y., Hoover, A., Villalba, R. M., Pavuluri, R., Smith, Y., & Dravid, S. M. (2020). Striatal glutamate delta-1 receptor regulates behavioral flexibility and thalamostriatal connectivity. *Neurobiology of Disease*, *137*, 104746. https://doi.org/10.1016/j.nbd.2020.104746

Miyamoto, Y., Katayama, S., Shigematsu, N., Nishi, A., & Fukuda, T. (2018). Striosome-based map of the mouse striatum that is conformable to both cortical afferent topography and uneven distributions of dopamine D1 and D2 receptor-expressing cells. *Brain Structure & Function*, *223*(9), 4275–4291. https://doi.org/10.1007/s00429-018-1749-3

Murray, R. C., Logan, M. C., & Horner, K. A. (2015). Striatal Patch Compartment Lesions Reduce Stereotypy Following Repeated Cocaine Administration. *Brain Research*, *1618*, 286–298. https://doi.org/10.1016/j.brainres.2015.06.012

Nakamoto, C., Kawamura, M., Nakatsukasa, E., Natsume, R., Takao, K., Watanabe, M., Abe, M., Takeuchi, T., & Sakimura, K. (2020). GluD1 knockout mice with a pure C57BL/6N background show impaired fear memory, social interaction, and enhanced depressive-like behavior. *PloS One*, *15*(2), e0229288. https://doi.org/10.1371/journal.pone.0229288

Nakamoto, C., Konno, K., Miyazaki, T., Nakatsukasa, E., Natsume, R., Abe, M., Kawamura, M., Fukazawa, Y., Shigemoto, R., Yamasaki, M., Sakimura, K., & Watanabe, M. (2020). Expression mapping, quantification, and complex formation of GluD1 and GluD2 glutamate receptors in adult mouse brain. *The Journal of Comparative Neurology*, *528*(6), 1003–1027. https://doi.org/10.1002/cne.24792

Nastase, S. A., Gazzola, V., Hasson, U., & Keysers, C. (2019). Measuring shared responses across subjects using intersubject correlation. *Social Cognitive and Affective Neuroscience*, *14*(6), 667–685. https://doi.org/10.1093/scan/nsz037

National Research Council (US) Committee for the Update of the Guide for the Care and Use of Laboratory Animals. (2011). *Guide for the Care and Use of Laboratory Animals* (8th ed.). National Academies Press (US). http://www.ncbi.nlm.nih.gov/books/NBK54050/

Nirenberg, M. J., Chan, J., Vaughan, R. A., Uhl, G. R., Kuhar, M. J., & Pickel, V. M. (1997). Immunogold Localization of the Dopamine Transporter: An Ultrastructural Study of the Rat Ventral Tegmental Area. *The Journal of Neuroscience*, *17*(11), 4037–4044. https://doi.org/10.1523/JNEUROSCI.17-11-04037.1997

Otsuka, S., Konno, K., Abe, M., Motohashi, J., Kohda, K., Sakimura, K., Watanabe, M., & Yuzaki, M. (2016). Roles of Cbln1 in Non-Motor Functions of Mice. *The Journal of*

Neuroscience: The Official Journal of the Society for Neuroscience, *36*(46), 11801–11816. https://doi.org/10.1523/JNEUROSCI.0322-16.2016

Pernice, H. F., Schieweck, R., Jafari, M., Straub, T., Bilban, M., Kiebler, M. A., & Popper, B. (2019). Altered Glutamate Receptor Ionotropic Delta Subunit 2 Expression in Stau2-Deficient Cerebellar Purkinje Cells in the Adult Brain. *International Journal of Molecular Sciences*, *20*(7). https://doi.org/10.3390/ijms20071797

Peters, A., Palay, S., & Webster, H. (1991). *The Fine Structure of the Nervous System* (3rd ed.). Oxford University Press.

Ragsdale, C. W., & Graybiel, A. M. (1991). Compartmental organization of the thalamostriatal connection in the cat. *The Journal of Comparative Neurology*, *311*(1), 134–167. https://doi.org/10.1002/cne.903110110

Raju, D. V., Ahern, T. H., Shah, D. J., Wright, T. M., Standaert, D. G., Hall, R. A., & Smith, Y. (2008). Differential synaptic plasticity of the corticostriatal and thalamostriatal systems in an MPTP-treated monkey model of parkinsonism. *European Journal of Neuroscience*, *27*(7), 1647–1658. https://doi.org/10.1111/j.1460-9568.2008.06136.x

Roberts, R. C., & Knickman, J. K. (2002). The ultrastructural organization of the patch matrix compartments in the human striatum. *The Journal of Comparative Neurology*, *452*(2), 128–138. https://doi.org/10.1002/cne.10351

Roberts, R. C., Roche, J. K., & Conley, R. R. (2005). Synaptic differences in the patch matrix compartments of subjects with schizophrenia: A postmortem ultrastructural study of the striatum. *Neurobiology of Disease*, *20*(2), 324–335. https://doi.org/10.1016/j.nbd.2005.03.015

Sadikot, A. F., Parent, A., & François, C. (1990). The centre médian and parafascicular thalamic nuclei project respectively to the sensorimotor and associative-limbic striatal territories in the squirrel monkey. *Brain Research*, *510*(1), 161–165. https://doi.org/10.1016/0006-8993(90)90746-x

Saunders, A., Macosko, E., Wysoker, A., Goldman, M., Krienen, F., de Rivera, H., Bien, E., Baum, M., Wang, S., Goeva, A., Nemesh, J., Kamitaki, N., Brumbaugh, S., Kulp, D., & McCarroll, S. A. (2018). Molecular Diversity and Specializations among the Cells of the Adult Mouse Brain. *Cell*, *174*(4), 1015-1030.e16. https://doi.org/10.1016/j.cell.2018.07.028

Seigneur, E., & Südhof, T. C. (2018). Genetic Ablation of All Cerebellins Reveals Synapse Organizer Functions in Multiple Regions Throughout the Brain. *The Journal of Neuroscience*, *38*(20), 4774–4790. https://doi.org/10.1523/JNEUROSCI.0360-18.2018

Shepherd, G. M. G. (2013). Corticostriatal connectivity and its role in disease. *Nature Reviews Neuroscience*, *14*(4), 278–291. https://doi.org/10.1038/nrn3469

Smith, J. B., Klug, J. R., Ross, D. L., Howard, C. D., Hollon, N. G., Ko, V. I., Hoffman, H., Callaway, E. M., Gerfen, C. R., & Jin, X. (2016). Genetic-Based Dissection Unveils the Inputs and Outputs of Striatal Patch and Matrix Compartments. *Neuron*, *91*(5), 1069–1084. https://doi.org/10.1016/j.neuron.2016.07.046

Smith, Y., Galvan, A., Ellender, T. J., Doig, N., Villalba, R. M., Huerta-Ocampo, I., Wichmann, T., & Bolam, J. P. (2014). The thalamostriatal system in normal and diseased states. *Frontiers in Systems Neuroscience*, *8*, 5. https://doi.org/10.3389/fnsys.2014.00005

Suryavanshi, P. S., Gupta, S. C., Yadav, R., Kesherwani, V., Liu, J., & Dravid, S. M. (2016). Glutamate Delta-1 Receptor Regulates Metabotropic Glutamate Receptor 5 Signaling in the Hippocampus. *Molecular Pharmacology*, *90*(2), 96–105. https://doi.org/10.1124/mol.116.104786

Tajima, K., & Fukuda, T. (2013). Region-specific diversity of striosomes in the mouse striatum revealed by the differential immunoreactivities for mu-opioid receptor, substance P, and enkephalin. *Neuroscience*, *241*, 215–228. https://doi.org/10.1016/j.neuroscience.2013.03.012

Tao, W., Díaz-Alonso, J., Sheng, N., & Nicoll, R. A. (2018). Postsynaptic δ1 glutamate receptor assembles and maintains hippocampal synapses via Cbln2 and neurexin. *Proceedings of the National Academy of Sciences of the United States of America*, *115*(23), E5373–E5381. https://doi.org/10.1073/pnas.1802737115

Tao, W., Ma, C., Bemben, M. A., Li, K. H., Burlingame, A. L., Zhang, M., & Nicoll, R. A. (2019). Mechanisms underlying the synaptic trafficking of the glutamate delta receptor GluD1. *Molecular Psychiatry*, *24*(10), 1451–1460. https://doi.org/10.1038/s41380-019-0378-4

Treutlein, J., Mühleisen, T. W., Frank, J., Mattheisen, M., Herms, S., Ludwig, K. U., Treutlein, T., Schmael, C., Strohmaier, J., Bösshenz, K. V., Breuer, R., Paul, T., Witt, S. H., Schulze, T. G., Schlösser, R. G. M., Nenadic, I., Sauer, H., Becker, T., Maier, W., … Rietschel, M. (2009). Dissection of phenotype reveals possible association between schizophrenia and Glutamate Receptor Delta 1 (GRID1) gene promoter. *Schizophrenia Research*, *111*(1–3), 123–130. https://doi.org/10.1016/j.schres.2009.03.011

Uchigashima, M., Cheung, A., Suh, J., Watanabe, M., & Futai, K. (2019). Differential expression of neurexin genes in the mouse brain. *Journal of Comparative Neurology*, *527*(12), 1940–1965. https://doi.org/10.1002/cne.24664

Uemura, T., Lee, S.-J., Yasumura, M., Takeuchi, T., Yoshida, T., Ra, M., Taguchi, R., Sakimura, K., & Mishina, M. (2010). Trans-Synaptic Interaction of GluRδ2 and Neurexin through Cbln1 Mediates Synapse Formation in the Cerebellum. *Cell*, *141*(6), 1068–1079. https://doi.org/10.1016/j.cell.2010.04.035

Unzai, T., Kuramoto, E., Kaneko, T., & Fujiyama, F. (2017). Quantitative Analyses of the Projection of Individual Neurons from the Midline Thalamic Nuclei to the Striosome and Matrix

Compartments of the Rat Striatum. *Cerebral Cortex (New York, N.Y.: 1991)*, *27*(2), 1164–1181. https://doi.org/10.1093/cercor/bhv295

Villasana, L. E., Klann, E., & Tejada-Simon, M. V. (2006). Rapid isolation of synaptoneurosomes and postsynaptic densities from adult mouse hippocampus. *Journal of Neuroscience Methods*, *158*(1), 30–36. https://doi.org/10.1016/j.jneumeth.2006.05.008

Wei, P., Pattarini, R., Rong, Y., Guo, H., Bansal, P. K., Kusnoor, S. V., Deutch, A. Y., Parris, J., & Morgan, J. I. (2012). The Cbln family of proteins interact with multiple signaling pathways. *Journal of Neurochemistry*, *121*(5), 717–729. https://doi.org/10.1111/j.1471-4159.2012.07648.x

Yuzaki, M. (2011). Cbln1 and its family proteins in synapse formation and maintenance. *Current Opinion in Neurobiology*, *21*(2), 215–220. https://doi.org/10.1016/j.conb.2011.01.010

Yuzaki, M. (2018). Two Classes of Secreted Synaptic Organizers in the Central Nervous System. *Annual Review of Physiology*, *80*(1), 243–262. https://doi.org/10.1146/annurev-physiol-021317-121322

Ziskin, J. L., Nishiyama, A., Rubio, M., Fukaya, M., & Bergles, D. E. (2007). Vesicular release of glutamate from unmyelinated axons in white matter. *Nature Neuroscience*, *10*(3), 321–330. https://doi.org/10.1038/nn1854